05,12

Investigation of magnetic correlations in aggregates of superparamagnetic particles in $NiFe_2O_4$ powders using ferromagnetic resonance

© S.V. Stolyar[1,2], I.G. Vazhenina[3,¶], A.O. Shokhrina[1,2], E.D. Nikolaeva[2], O.A. Li[1,2], R.S. Iskhakov[3], A.V. Belyi[2]

[1] Siberian Federal University, Krasnoyarsk, Russia
[2] Federal Research Center „Krasnoyarsk Scientific Center Siberian Branch of the Russian Academy of Sciences", Krasnoyarsk, Russia
[3] Kirensky Institute of Physics, Federal Research Center KSC SB, Russian Academy of Sciences, Krasnoyarsk, Russia

¶ E-mail: irina-vazhenina@mail.ru

Received March 6, 2025
Revised March 6, 2025
Accepted May 5, 2025

In order to establish the effect of magnetic interparticle interactions on the dynamic properties of a powder system of superparamagnetic nickel ferrite nanoparticles with an average size of ~ 4 nm, the temperature dependences of the ferromagnetic resonance (FMR) curve parameters were investigated and analyzed. To describe the experimental results obtained by the FMR method, a model of random magnetic anisotropy is used, which considers the effect of magnetic interparticle interactions on the value of the effective anisotropy constant in an external field. The analysis showed the presence of strong magnetic interactions in the studied system, which disappear when the temperature rises above the blocking temperature and allowed us to obtain quantitative estimates of the intensity and energy of magnetic interparticle interactions, as well as to determine the magnetic anisotropy constant of individual particles (without taking into account the influence of magnetic interparticle interactions).

Keywords: nickel ferrite nanoparticles, ferromagnetic resonance, superparamagnetism, interparticle interaction, length of magnetic correlations

DOI: 10.61011/PSS.2025.07.61890.30HH-25

1. Introduction

Nanometer-range powders (particle size $d < 10$ nm) exhibit a wide variety of properties and physical effects not typical of massive analogues [1–4]. The features of magnetic powder materials are primarily related to the developed specific surface area, where magnetically active atoms are in a different environment than that of magnetically active atoms inside the particle. Therefore, the surface will be characterized by its own set of magnetic parameters: K_S — surface anisotropy, M_S — magnetization, T_S — magnetic disordering temperature. The next important feature of powder systems is superparamagnetism. This state occurs when the energy of the magnetic anisotropy of a particle becomes less than the thermal energy

$$KV \leq k_{\mathrm{B}} T_B, \tag{1}$$

where T_B is the blocking temperature, V is the particle volume, k_{B} is the Boltzmann constant. The magnetic anisotropy constant of the particle K here is formed from the anisotropy constant of the particle core K_V and the contribution K_S due to the surface

$$K = K_V + 6K_S/d. \tag{2}$$

An important feature of powder systems is also the magnetic interparticle interaction [5,6]. As a result of this interaction, the magnetic moments of the particles in a certain volume will behave correlated, forming a magnetic block of size L, which depends on the magnetic field H and is characterized by magnetization M

$$L(H) = d + \left(2A/(MH + C)\right)^{1/2}. \tag{3}$$

The parameter A has the same meaning in this expression as the exchange constant for nanocrystalline alloys. The parameter C characterizes the interparticle interactions [7,8].

The average value of the anisotropy constant of the magnetic block is obtained by averaging over N particles within the correlation volume

$$\langle K \rangle = K/N^{1/2}, \tag{4}$$

where N is the number of particles in the magnetic block. The intensity of the interparticle interaction can be eliminated or weakened by coating the particles or placing them in a non-magnetic matrix [9].

The effect of interparticle interaction is most pronounced when determining the blocking temperature T_B by measuring $M(T)$ using the protocols ZFC (zero external field

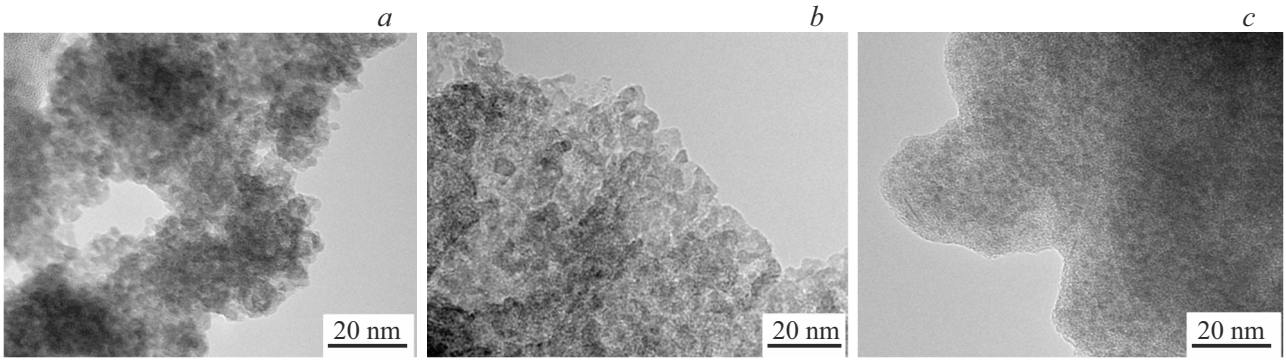

Figure 1. Images of powders of $NiFe_2O_4$ (a), $NiFe_2O_4$/SDS (b) and $NiFe_2O_4$/PVA (c) obtained with a transmission electron microscope.

cooling) and FC (external field cooling). The values of T_B depend on the magnitude of the external magnetic field H [6,10,11], an increase in which causes a decrease in L and, according to (1), a decrease in T_B. The change in the shape of the dependence $T_B(H)$ from that characteristic of a powder with interparticle interaction to that characteristic of a powder without interparticle interaction with an increase in the magnetic field occurs at a field value at which $L \to d$ [8].

The ferromagnetic resonance (FMR) method is a simple and reliable method for studying the properties of magnetic materials. The FMR phenomenon is caused by the absorption of microwave field energy when the frequency of the microwave field ω coincides with the frequency of precession of the magnetization vector around the direction of the effective magnetic field $\mathbf{H}_{eff}$. The macroscopic description of FMR is given by the Landau–Lifshitz–Gilbert equation [12]

$$\dot{\mathbf{M}} = -\gamma \mathbf{M} \times \mathbf{H}_{eff} - \gamma \frac{\alpha}{M} \mathbf{M} \times (\mathbf{M} \times \mathbf{H}_{eff}), \qquad (5)$$

where $\mathbf{M}$ is the instantaneous value of the magnetization vector, γ is the gyromagnetic ratio, α is the attenuation parameter. The field $\mathbf{H}_{eff}$, in the simplest case, consists of the external field $\mathbf{H}$, the internal anisotropy field $\mathbf{H}_K$ of the ferromagnet and the demagnetizing field of the sample. For a spherical massive sample, the resonance condition is determined by the ratio $\omega = \gamma H$, and the width of the FMR line $\Delta H = 2\alpha H$. The FMR method has already proven itself in the study of magnetic powders [13].

This paper presents experimental results of temperature studies of ferromagnetic resonance of nickel ferrite powder systems with interparticle interaction. The purpose of the paper is to demonstrate the effects of interparticle interaction in magnetodynamic studies, as well as to determine the magnetic parameters of powders K, A_{eff}, L, characterizing magnetic interparticle interaction.

2. Experimental methodology

Magnetic nanoparticles doped with nickel were obtained by chemical co-deposition. Salts of $NiSO_4 \cdot 7H_2O$ and $FeCl_3 \cdot 6H_2O$ in the molar ratio 1:2 were dissolved in 100;ml dH_2O, in 0.1 % solution of dodecyl sulfate Na (SDS) or 0.1 % solution of polyvinyl alcohol (PVA), stirred until all components were completely dissolved and then 10 ml of NH_4OH (up to pH = 11) was added, kept with constant stirring for 30 minutes. The resulting precipitate was washed and dried in a drying cabinet at a temperature of 60 °C. The resulting material was ground in a mortar. Microphotographs were taken with a Hitachi HT7700 transmission electron microscope. The ImageJ program was used to obtain particle size data. The area of the particle was selected using the „oval selection“ tool, after which its area was fixed, and then recalculated into diameter using the formula $S = \pi(d/2)^2$. The average ratio of the semiaxes of the particle regions was 0.94, 1.07, 1.05 for samples $NiFe_2O_4$, $NiFe_2O_4$/SDS, $NiFe_2O_4$/PVA, respectively, which makes it possible to model the shape of the particles as spherical. The data obtained was processed using the capabilities of the Python programming language (Matplotlib, Seaborn, and SciPy libraries). When constructing frequency histograms, the column width was 1 nm, the plot area was from 0.5 to 10.5 nm. The magnetization measurements were carried out on a vibrating magnetometer [14].

The ferromagnetic resonance (FMR) curves were recorded on the equipment of Krasnoyarsk Regional Common Use Center of the Federal Research Center Krasnoyarsk Science Center of the Siberian Branch of the Russian Academy of Sciences (ELEXSYS E580 spectrometer, Bruker, Germany) at pumping frequency of resonant cavity $f = 9.48$ GHz in the temperature range from 20 to 300 K.

3. Results and discussion

Figure 1 shows images of aggregate nanoparticles obtained using a transmission electron microscope. The particles had a shape close to spherical. Figure 2 shows the histograms of the particle size distribution of the studied powders. The average size d does not depend on the wetting coating for all synthesized powders ($NiFe_2O_4$, $NiFe_2O_4$/SDS, $NiFe_2O_4$/PVA) had a value of about 4 nm.

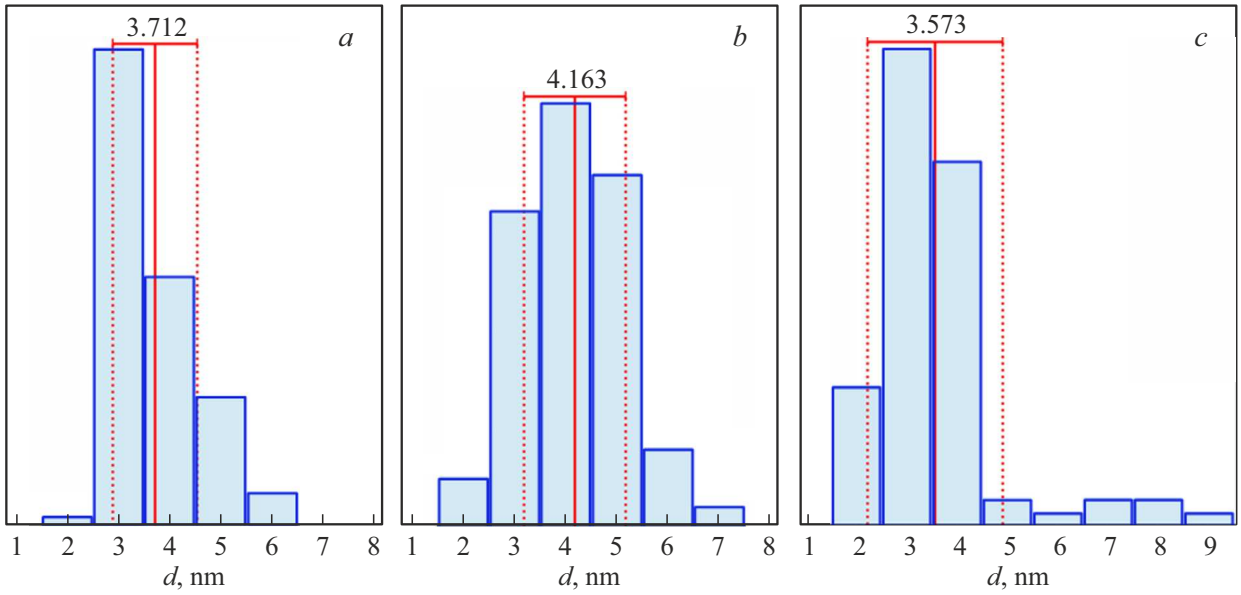

Figure 2. Histograms of the particle size distribution of the studied powders $NiFe_2O_4$ (a), $NiFe_2O_4$/SDS (b) and $NiFe_2O_4$/PVA (c).

The above photographs of the powders convincingly demonstrate that particles do not contact each other in the powder of $NiFe_2O_4$/PVA and are located at distances of several d from each other. We will consider this powder to be a system with no interparticle interaction. The powder nanoparticles come into contact with their neighbors for the uncoated powder of $NiFe_2O_4$, as can be seen in Figure 1, a. This powder will be considered as a system with the presence of interparticle magnetic interaction. An intermediate state is realized in the powder of $NiFe_2O_4$/SDS, therefore, this powder will be considered a system with insignificant interparticle magnetic interaction between nanoparticles. Figure 3 shows the magnetization curves of powders at $T = 4.2$ K and $T = 100$ K, as well as hysteresis loops recorded at $T = 4.2$ K. It can be seen from the curves that the magnetization of powders in the 3 kOe field at $T = 100$ K is ~ 3.5 emu/g. Figure 4 shows the characteristic differential absorption curves of microwave field energy (FMR curves) of manufactured powders of $NiFe_2O_4$, $NiFe_2O_4$/SDS, $NiFe_2O_4$/PVA measured at different temperatures.

The parameters determined from the experimental FMR curves are the resonance field H_{res} and the line width ΔH, the temperature dependences of which are shown in Figs. 5 and 6, respectively. The temperature dependences of the intensity I of the FMR resonance curve for each synthesized powder, which was determined as the product of the line width ΔH and the height of the differential absorption curve dP/dH ($I = \Delta H \cdot dP/dH$), are shown in Figure 7.

As can be seen from the curves in Figure 7, the temperature dependences of the FMR intensity of the manufactured powders have a similar appearance — blurred by the maximum at temperatures of 200, 150 and 80 K for powders of $NiFe_2O_4$, $NiFe_2O_4$/SDS, $NiFe_2O_4$/PVA, respectively. The position of the maximum correlates with our reasoning based on the analysis of powder images (see Figure 1). The presence of interparticle interaction leads to an increase in temperature, at which the intensity is maximum. The width of the observed maxima $I(T)$ also correlates with the intensity of interparticle interaction of powders. Curves on Figure 7 show that there is a shift of the maximum point in the ratio $T(NiFe_2O_4/PVA) < T(NiFe_2O_4/SDS) < T(NiFe_2O_4)$. Thus, the presence of a magnetic interaction between the powder particles affects the parameters of the FMR.

Temperature dependences $I(T)$ were observed in composite systems γ-Fe_2O_3/SiO_2 [15], in superparamagnetic nanoparticles γ-Fe_2O_3, encapsulated in second-generation liquid crystal dendrimers [16], in magnetic magnetite nanoparticles γ-Fe_2O_3/SiO_2 [17], in ferrihydrite nanoparticles [18]. In these studies, the observed maximum based on the temperature dependence $I(T)$ was associated with the superparamagnetic blocking temperature of the studied powders T_B, which is determined by the Neel–Brown ratio

$$T_B = KV/\ln(\tau_m/\tau_0)k_B, \tag{6}$$

where τ_m is the characteristic time of the experimental technique, τ_0 is the relaxation time of a particle whose magnitude is in the range 10^{-9}–10^{-13} s, V is the volume particles. The value of τ_m for static magnetic measurements varies from 10 to 100 s, for FMR $\tau_m \sim 1/f$ and at the frequency used is of the order of 10^{-12} s. Therefore, the ratio $T_B^{FMR}/T_B^{M(T)} \approx 4$–$5$ must be observed between the blocking temperature determined from FMR T_B^{FMR} and the same parameter determined from static magnetic measurements $T_B^{M(T)}$. Since $T_B^{M(T)}$ of the studied powder of $NiFe_2O_4$ is about 40 K [8], T_B^{FMR} should take values from

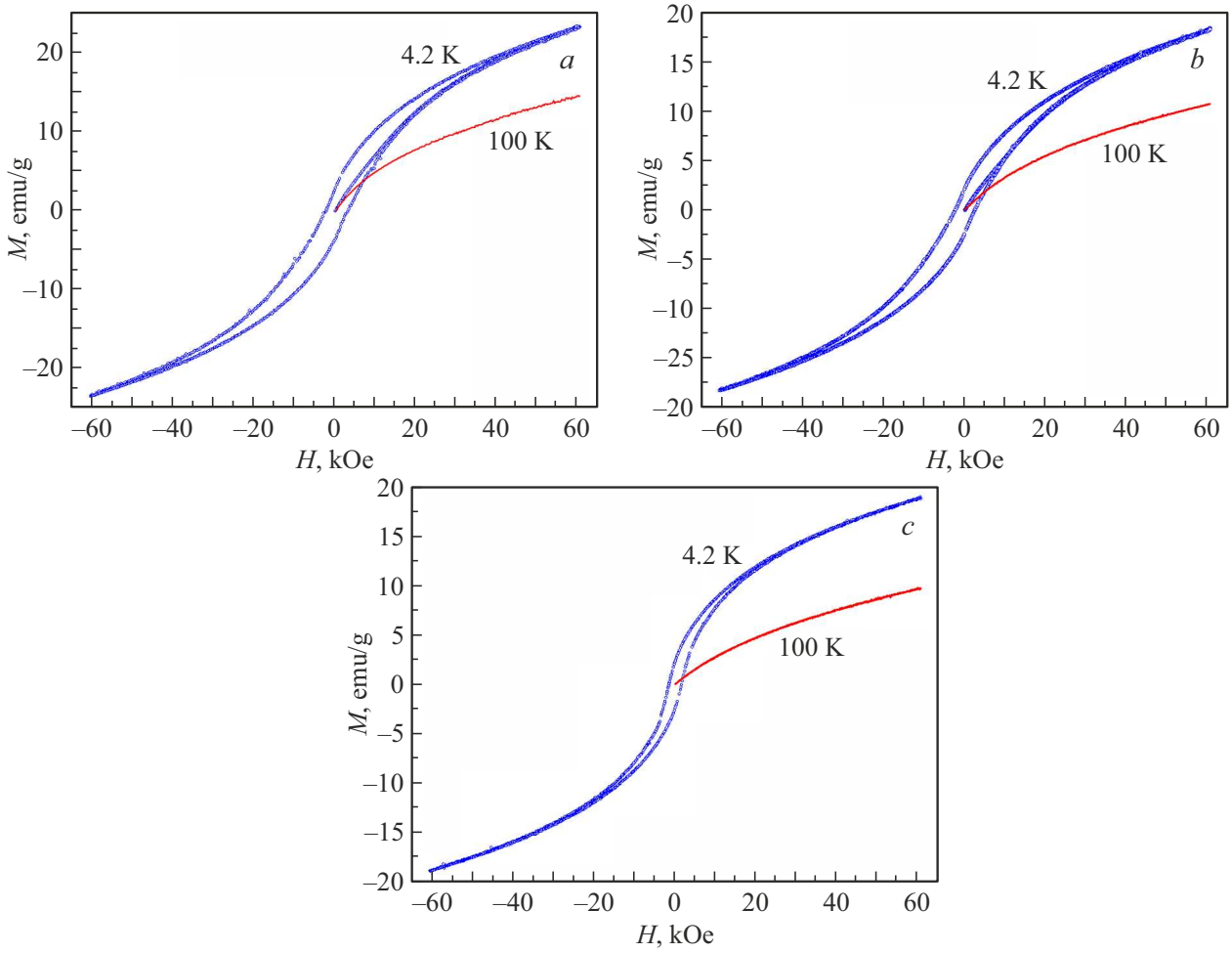

Figure 3. Magnetization curves at 4.2 K and 100 K for three different powders $NiFe_2O_4$ (a), $NiFe_2O_4$/SDS (b) and $NiFe_2O_4$/PVA (c).

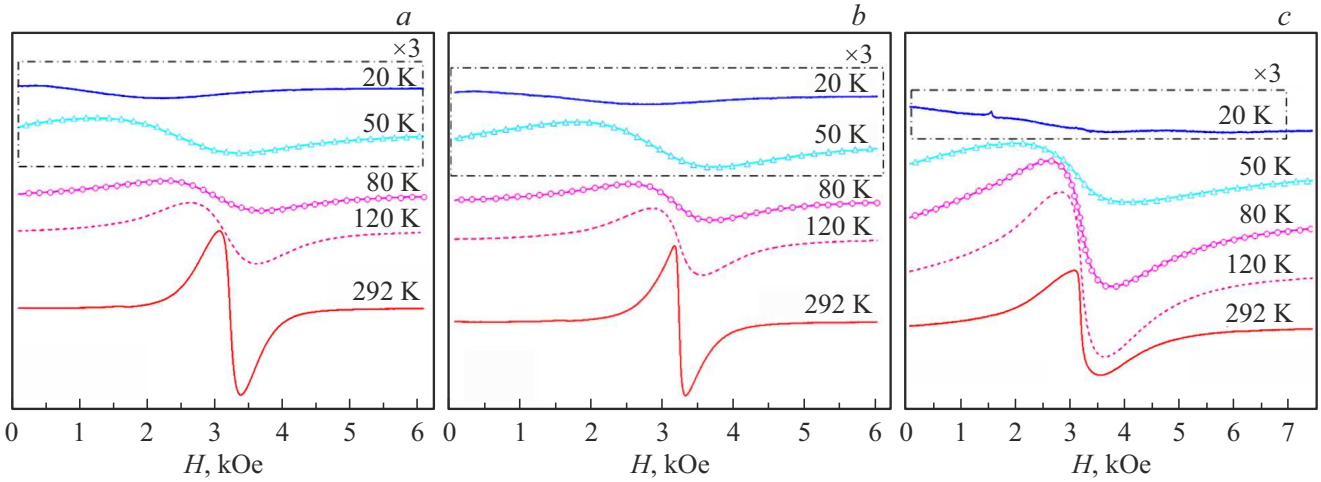

Figure 4. Examples of experimental FMR spectra at different temperatures for three different powders of $NiFe_2O_4$ (a), $NiFe_2O_4$/SDS (b) and $NiFe_2O_4$/PVA (c).

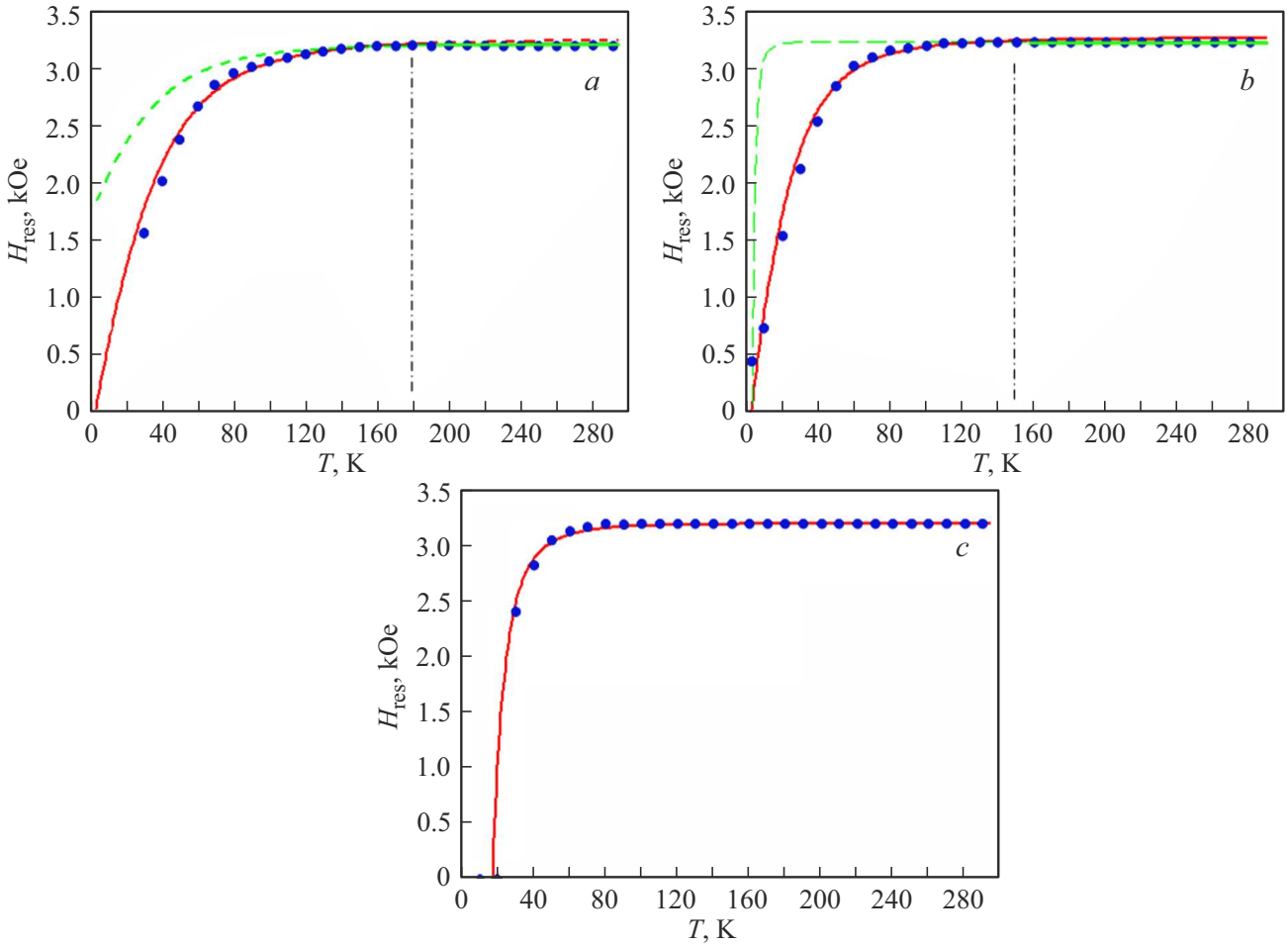

Figure 5. Temperature dependences of experimental values of the resonance field H_{res} (dots) and calculated curves (dotted and solid lines) of powders of $NiFe_2O_4$ (a), $NiFe_2O_4$/SDS (b) and $NiFe_2O_4$/PVA (c).

160 to 200 K. According to Figure 7, and T_B^{FMR} for $NiFe_2O_4$ is 200 K, thus, the values of $T_B^{M(T)}$ and T_B^{FMR} estimated from the magnetic static and dynamic measurements are in good agreement. The values of T_B^{FMR} for our powders $NiFe_2O_4$/SDS and $NiFe_2O_4$/PVA (Figure 7, b and c) are equal to 150 and 80 K, respectively.

To analyze the temperature dependences of the resonance field $H_{res}(T)$ and the line width $\Delta H(T)$ of the manufactured powders, we use the results of Reicher–Stepanov theory [19–22], in which the ferromagnetic resonance of superparamagnetic powders is considered. According to the cited papers, in powders of chaotically oriented particles of ferromagnets and ferrites, the absorption line width turns out to be a nonmonotonic function of temperature

$$\Delta H(T) = \Delta H_S(T) + \Delta H_U(T), \qquad (7)$$

where $\Delta H_S(T)$ is the contribution to broadening due to superparamagnetism of nanoparticles, $\Delta H_U(T)$ is the contribution to broadening due to the spread of directions of particle anisotropy fields (inhomogeneous broadening), which is decisive at low temperatures. The temperature dependence $\Delta H(T)$, taking into account that $\Delta H_S(T)$ and $\Delta H_U(T)$ are functions of the Langevin parameter $\xi_0 = (\omega/\gamma) \cdot (MV/k_{\mathrm{B}}T)$, can be represented by the expression

$$\Delta H(T) = \frac{2}{\sqrt{3}} \frac{\omega}{\gamma} \frac{\alpha(\xi_0 - L_1)}{\xi_0 \cdot L_1} + 3 \frac{\omega}{\gamma} \frac{\varepsilon \cdot L_2}{L_1}, \qquad (8)$$

where $L_1 = \coth \xi_0 - (1/\xi_0)$ and $L_2 = 1 - (3L_1/\xi_0)$ are Langevin functions, $\varepsilon = K\gamma/M\omega$, the attenuation parameter α was assumed to be 0.01, $\gamma = 1.8 \cdot 10^7$ Hz/Oe [23].

Temperature dependence of the resonant field $H_{res}(T)$, according to Ref. [20], is described by the following expression

$$H_{res}(T) = \frac{\omega}{\gamma} \left[1 - 2\varepsilon_A \frac{(\xi_0 - 3L_1)^2}{\xi_0^3 \cdot L_1} \right], \qquad (9)$$

where $\varepsilon_A = KV/k_{\mathrm{B}}T$.

Fitting curves of temperature dependences $H_{res}(T)$ and $\Delta H(T)$ were obtained using expressions (8) and (9) and are shown in Figures 5 and 6 with dotted and solid lines. The fitting parameters d, M, K of the calculated curves are shown in the table. For powder of $NiFe_2O_4$/PVA

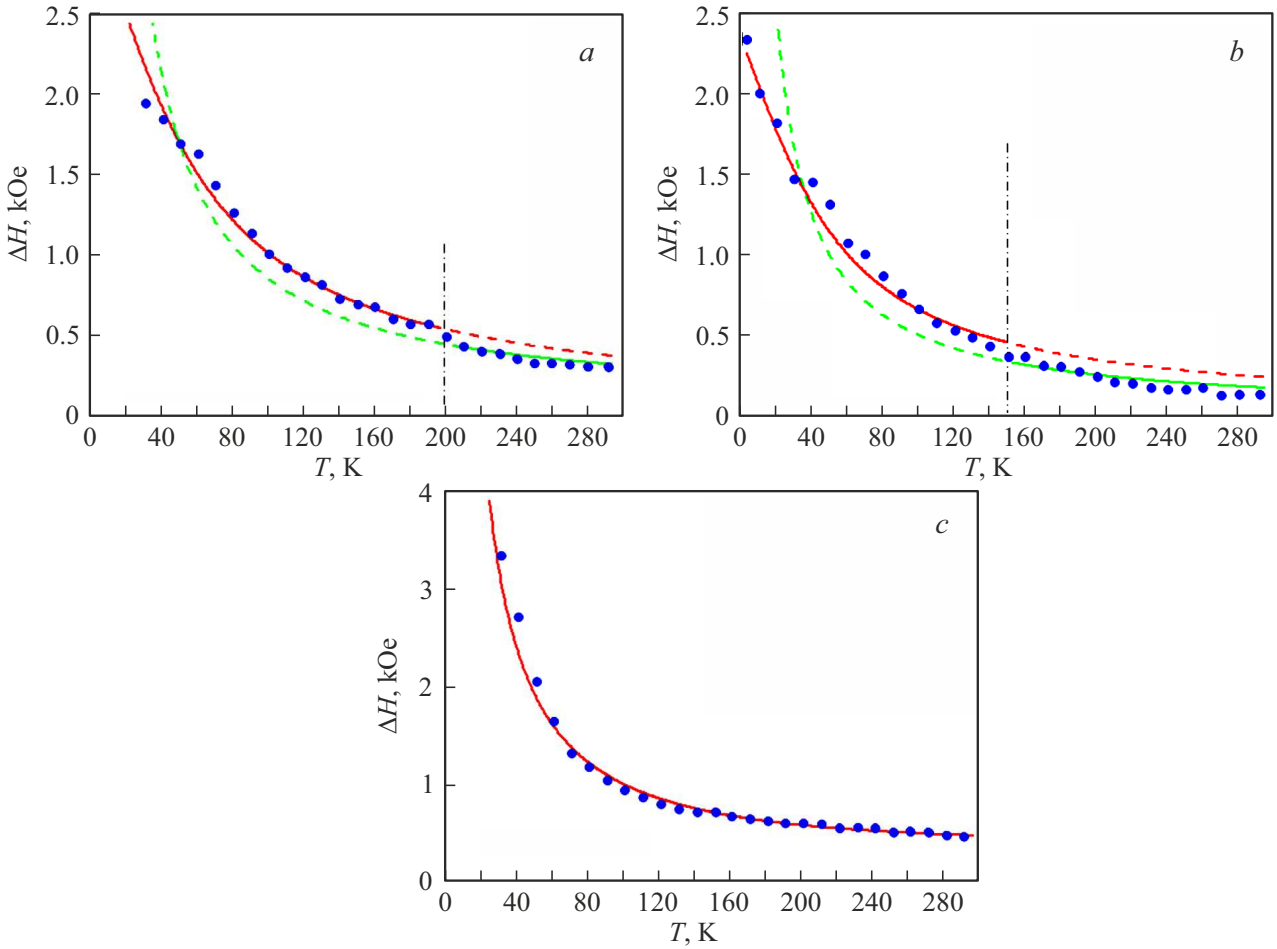

Figure 6. Temperature dependences of experimental line widths ΔH (dots) and calculated curves (dotted and solid lines) of powders of $NiFe_2O_4$ (*a*), $NiFe_2O_4$/SDS (*b*) and $NiFe_2O_4$/PVA (*c*).

Powder parameters determined from calculated FMR curves

Powder type, temperature range		$NiFe_2O_4$		$NiFe_2O_4$/SDS		$NiFe_2O_4$/PVA
		$20 < T \leq 180$ K	$180 \leq T < 300$ K	$20 < T \leq 150$ K	$150 \leq T < 300$ K	$20 < T < 300$ K
d, nm	from $H_{res}(T)$	10	4	8	4	5.5
	from $\Delta H(T)$	10	4	8	4	4
M, G	from $H_{res}(T)$	13	9	19	9	20
	from $\Delta H(T)$	13	9	22	8	18
$\langle K \rangle \cdot 10^5$, erg/cm^3	from $H_{res}(T)$	0.22		0.34		$\langle K \rangle = K = 2.1$
	from $\Delta H(T)$	0.14		0.21		
$K \cdot 10^5$, erg/cm^3	from $H_{res}(T)$		1.7		1.2	
	from $\Delta H(T)$		1.7		1.2	

with minimum blocking temperature of $T_B^{\mathrm{FMR}} = 80$ K and absence of interparticle interaction, the fitting parameters $d = 4$ nm and $M = 18$ G are consistent with the results of microscopic studies and the magnitude of magnetization estimated based on magnetic static measurement data (see Figures 1–3). The value of the anisotropy constant $K \approx 2 \cdot 10^5$ erg/cm^3, used to construct the fitting curve, also has a reasonable value and is comparable to the results [8]. It should be noted that both $H_{res}(T)$ and $\Delta H(T)$ for powder of $NiFe_2O_4$/PVA are described by a theoretical

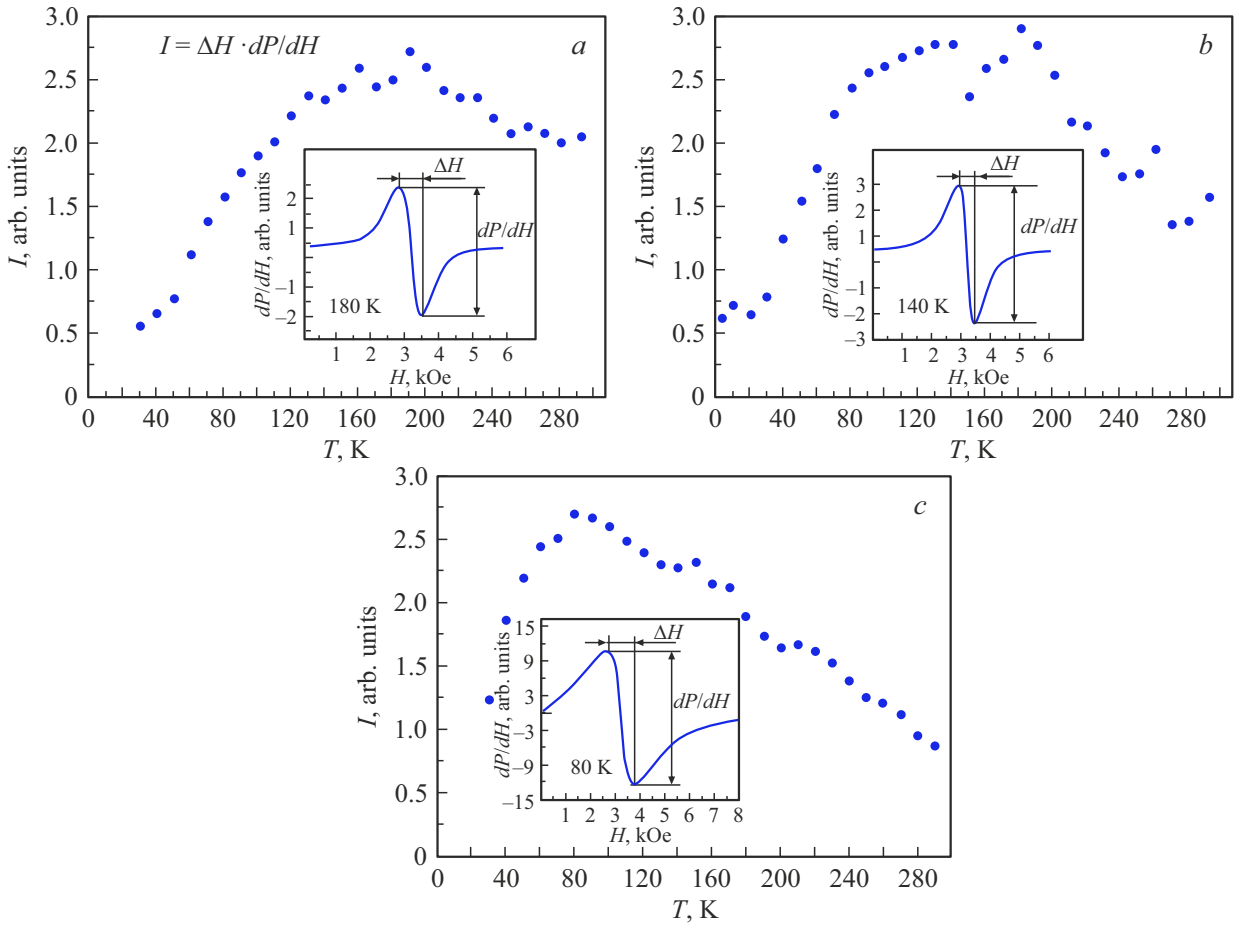

Figure 7. Temperature dependences of experimental intensity values I of powders of $NiFe_2O_4$ (a), $NiFe_2O_4$/SDS (b) and $NiFe_2O_4$/PVA (c).

curve requiring only one set of parameters d, M, K over the entire temperature range. Thus, the change of state from ferromagnetic to superparamagnetic at the blocking temperature did not manifest itself on the fitting curves $H_{res}(T)$ and $\Delta H(T)$ of this powder.

Experimental dependences $H_{res}(T)$ and $\Delta H(T)$ of powders of $NiFe_2O_4$ and $NiFe_2O_4$/SDS with interparticle interaction cannot be adjusted using a single set of parameters d, M, K. The areas of the blocked and unblocked states $T < T_B^{\mathrm{FMR}}$ and $T > T_B^{\mathrm{FMR}}$ are characterized by a different set of adjustable parameters d, M, K (see the table). Moreover, the transition through the blocking temperature T_b^{FMR} is accompanied by a decrease in the particle size d and an increase in the anisotropy constant K.

Particle size $d = 4$ nm, used for the fitting curve of powders $NiFe_2O_4$ and $NiFe_2O_4$/SDS with interparticle interaction in the unblocked state $T > T_B^{\mathrm{FMR}}$, consistent with the results of electron microscopy. The value of d in the blocked state is 2–3 times the particle size of the powders. This is due to the fact that the adjustment parameter d for $T < T_B^{\mathrm{FMR}}$ characterizes the size of the correlation magnetic block L. By comparing the fitting parameters of the resonance curves of the powder $NiFe_2O_4$ with the maximum interparticle interaction, it is possible to determine the number of nanoparticles included in the magnetic block, $N = V_L/V$. Considering that the ratio of the volumes of the magnetic block V_L and the nanoparticle V is estimated as the cube of the ratio of their characteristic sizes, with the size of the magnetic block $d = L = 10$ nm and the size of the nanoparticle $d = 4$ nm we get $N = 15$ particles.

The fitting values of the magnetic anisotropy constant K powder $NiFe_2O_4$ obtained from the dependencies $H_{res}(T)$ and $\Delta H(T)$ for the locked state $T < T_B^{\mathrm{FMR}}$ characterize the anisotropy constant of the magnetic block $\langle K \rangle$. The estimate of its value (defined as the arithmetic mean) gives the value $\langle K \rangle \approx 0.23 \cdot 10^5$ erg/cm^3. Following a similar procedure for the anisotropy constant of a particle, we can write $K = 1.6 \cdot 10^5$ erg/cm^3. Their ratio is $K/\langle K \rangle \approx 7$. The latter does not contradict the relation (4), which establishes the relationship between the anisotropy constant of the magnetic block and the anisotropy constant of the particle.

It should be noted that initially the model of random anisotropy or ripples of magnetization was developed to explain the properties of amorphous and nanocrystalline alloys. The length of the magnetic correlations or the size

of the magnetic block L and the average constant of the magnetic anisotropy of this block are related by the ratio in this model: $A = \langle K \rangle L^2$. Using the results obtained above $\langle K \rangle \approx 0.23 \cdot 10^5$ erg/cm^3, $L = 10$ nm, it is possible to estimate the parameter A: $A = 230 \cdot 10^{-10}$ erg/cm. Using (3), it is possible to estimate the parameter C, which characterizes the intensity of interparticle magnetic interactions between nanoparticles. Assuming $M = 20$ G, the magnetic field $H = 3.3$ kOe for FMR measurements at a frequency of 9.48 GHz, $d = 4$ nm, we obtain $C \approx 6 \cdot 10^4$ erg/cm^3. The obtained values of A and C are consistent with the results of Ref. [8], which studied the field dependences of the blocking temperature $T_B(H)$ using measurements $M(T)$ with ZFC and FC for powders of $NiFe_2O_4$.

Conclusion

Nickel ferrite powders with a nanoparticle size of ~ 4 nm were produced by chemical deposition with different types of coating: uncoated nanoparticles — powders $NiFe_2O_4$; nanoparticle powders $NiFe_2O_4$/SDS coated with dodecyl sulfate Na (SDS); powders of $NiFe_2O_4$/PVA nanoparticles coated with polyvinyl alcohol (PVA). The different type of coating caused the different intensity of the magnetic interparticle interaction. The temperature dependences of the ferromagnetic resonance curve parameters (resonance field H_{res}, line width ΔH, and intensity I) for the manufactured powders are studied. The temperature dependences of the resonance absorption intensity $I(T)$ allowed determining the blocking temperatures T_B^{FMR} of powders, which for $NiFe_2O_4$, $NiFe_2O_4$/SDS, $NiFe_2O_4$/PVA are 200, 150 and 80 K, respectively. The values of T_B^{FMR} reflect the intensity of magnetic interparticle interactions. The temperature dependences of the resonant field $H_{res}(T)$ and the line width $\Delta H(T)$ were analyzed in the framework of Reicher–Stepanov theory [19–22]. It turned out that the calculated curves $H_{res}(T)$ and $\Delta H(T)$ of powders in the region of blocked ($T < T_B^{\mathrm{FMR}}$) and unblocked ($T > T_B^{\mathrm{FMR}}$) states are characterized by a different set of adjustable parameters d, $\langle K \rangle$, M (d is the magnetic conglomerate size, $\langle K \rangle$ is the magnetic anisotropy constant of the magnetic conglomerate, M is the magnetization). The transition through the blocking temperature (with an increase in temperature from 20 K to room values) in powders with magnetic interparticle interactions is accompanied by a decrease in the size of the magnetic conglomerate d from 10 to 4 nm and an increase in the parameter $\langle K \rangle$ c $0.23 \cdot 10^5$ erg/cm^3 to $1.6 \cdot 10^5$ erg/cm^3. The observed features reflect the influence of magnetic interparticle interactions between nanoparticles and are consistent with the model of random magnetic anisotropy, for which the anisotropy constant of the magnetic block (conglomerate) $\langle K \rangle$ and the anisotropy constant of the nanoparticle K are related by the ratio $\langle K \rangle = K/N^{1/2}$, where N is the number of particles in a magnetic conglomerate.

Acknowledgments

The authors would like to thank the Krasnoyarsk Regional Common Use Center of the Federal Research Center Krasnoyarsk Science Center of the Siberian Branch of the Russian Academy of Sciences for providing the equipment for measurements.

Funding

The study was carried out within the framework of the scientific topic of the State Assignment of the Krasnoyarsk Regional Common Use Center of the Federal Research Center Krasnoyarsk Science Center of the Siberian Branch of the Russian Academy of Sciences.

Conflict of interest

The authors declare that they have no conflict of interest.

References

[1] S.P. Gubin, Yu.A. Koksharev, G.B. Khomutov, G.Yu. Yurkov. Uspekhi khimii **74**, 539 (2005). (in Russian).
[2] S.H. Bossmann, H. Wang, eds. Magnetic Nanomaterials: Applications in Catalysis and Life Sciences. Royal Society of Chemistry, Cambridge (2017).
[3] G.F. Stiufiuc, R.I. Stiufiuc. Appl. Sci. **14**, 1623 (2024).
[4] D. Lisjak, A. Mertelj. Prog. Mater. Sci. **95**, 286 (2018).
[5] J.M. Vargas, W.C. Nunes, L.M. Socolovsky, M. Knobel, D. Zanchet. Phys. Rev. B **72**, 184428 (2005).
[6] M. Knobel, W.C. Nunes, H. Winnischofer, T.C.R. Rocha, L.M. Socolovsky, C.L. Mayorga, D. Zanchet. J. Non-Cryst. Solids **353**, 743 (2007).
[7] Y.V. Knyazev, D.A. Balaev, S.V. Stolyar, A.O. Shokhrina, D.A. Velikanov, A.I. Pankrats, A.M. Vorotynov, A.A. Krasikov, S.A. Skorobogatov, M.N. Volochaev, O.A. Bayukov, R.S. Iskhakov. J. Magn. Magn. Mater. **613**, 172675 (2025).
[8] D.A. Balaev, A.A. Krasikov, Yu.V. Knyazev, S.V. Stolyar, A.O. Shokhrina, A.D. Balaev, R.S. Iskhakov. Pis'ma v ZhETF **120**, *10*, 785 (2024). (in Russian).
[9] C. Binns, M.J. Maher, Q.A. Pankhurst, D. Kechrakos, K.N. Trohidou. Phys. Rev. B **66**, 184413 (2002).
[10] A.A. Krasikov, Y.V. Knyazev, D.A. Balaev, D.A. Velikanov, S.V. Stolyar, Y.L. Mikhlin, R.N. Yaroslavtsev, R.S. Iskhakov. Phys. B Condens. Matter. **660**, 414901 (2023).
[11] A.A. Krasikov, Yu.V. Knyazev, D.A. Balaev, S.V. Stolyar, V.P. Ladygina, A.D. Balaev, R.S. Iskhakov. ZhETF **164**, *6*, 1026 (2023). (in Russian).
[12] A.G. Gurevich, Magnitnyi rezonans v ferritakh i antiferomagnetikakh. Nauka, M. (1973). p. 591. (in Russian).
[13] I. Benguettat-El Mokhtari, D.S. Schmool. Magnetochemistry **9**, 191 (2023).
[14] A.D. Balaev, Yu.V. Boyarshinov, M.M. Karpenko, B.P. Khrustalev. PTE *3*, 167 (1985). (in Russian).
[15] R. Berger, J.-C. Bissey, J. Kliava, H. Daubric, C. Estournès. J. Magn. Magn. Mater. **234**, 535 (2001).
[16] N.E. Domracheva, A.V. Pyataev, R.A. Manapov, M.S. Gruzdev. ChemPhysChem. **12**, 3009 (2011).

[17] I.G. Vazhenina, S.V. Stolyar, A.V. Tyumentseva, M.N. Volochaev, R.S. Iskhakov, S.V. Komogortsev, V.F. Pyankov, E.D. Nikolaeva. FTT **65**, *6*, 923 (2023). (in Russian).
[18] M. Wencka, A. Jelen, M. Jagodič, V. Khare, C. Ruby, J. Dolinšek. J. Phys. D: Appl. Phys. **42**, 245301 (2009).
[19] Y.L. Reicher, M.I. Shliomis. ZhETF **67**, *3*, 1060 (1974). (in Russian).
[20] R.S. Geht, V.A. Ignatchenko, Y.L. Reicher, M.I. Shliomis. ZhETF **70**, *4*, 1300 (1976). (in Russian).
[21] Y.L. Raikher, V.I. Stepanov. ZhETF **102**, *4*, 1409 (1992). (in Russian).
[22] Y.L. Raikher, V.I. Stepanov. Phys. Rev. B **50**, 6250 (1994).
[23] S.V. Stolyar, O.A. Li, E.D. Nikolaeva, N.M. Boev, A.M. Vorotynov, D.A. Velikanov, R.S. Iskhakov, V.F. Pyankov, Yu.V. Knyazev, O.A. Bayukov, A.O. Shokhrina, M.S. Molokeev, A.D. Vasiliev. FTT **65**, 1006 (2023). (in Russian).

Translated by A.Akhtyamov